Deep Learning–Assisted Two-Dimensional Transperineal Ultrasound for Analyzing Bladder Neck Motion in Women With Stress Urinary Incontinence

Authors: Jin Wang, MD; Xin Yang, PhD; Yinnan Wu, MD, PhD; Yanqing Peng, MD; Yan Zou, MD; Xiduo Lu, MS; Shuangxi Chen, MD; Xiaoyi Pan, MS; Dong Ni, PhD; Litao Sun, MD, PhD

Affiliations: Cancer Center, Department of Ultrasound Medicine, Zhejiang Provincial People's Hospital, Affiliated People's Hospital of Hangzhou Medical College, Hangzhou, Zhejiang, China (Drs Wang, Peng, Zou, Chen, Wu and Sun); National-Regional Key Technology Engineering Laboratory for Medical Ultrasound, School of Biomedical Engineering, Shenzhen University, Shenzhen, China (Mr Yang and Mr Ni); School of Mathematical Sciences, Zhejiang University, Zijingang Campus, Hangzhou, Zhejiang, China (Dr Wu); Medical UltraSound Image Computing (MUSIC) Lab, Shenzhen University, China (Mr Yang and Mr Ni); Shenzhen RayShape Medical Technology Co., Ltd, Shenzhen, China (Ms Lu and Ms Pan).

J.W. and X.Y. contributed equally to this study.

Corresponding authors:

Litao Sun, MD, PhD

Address: Department of Ultrasound Medicine, Zhejiang Provincial People's Hospital, Affiliated People's Hospital of Hangzhou Medical College, 158 Shangtang Road, Hangzhou 310014, China;

Email: litaosun1971@sina.com

Phone: +8615158110363;

Dong Ni, PhD

Address: National-Regional Key Technology Engineering Laboratory for Medical Ultrasound, Shenzhen University, 1066 Xueyuan Road, Shenzhen 518073, China; Email: nidong@szu.edu.cn

Phone: +8613928464070

Disclosure statement: The authors report no conflict of interest.

Financial support: The authors received no specific funding for this study and declare that they have no known competing financial interests or personal relationships that could have appeared to influence the work reported in this paper.

Word count: abstract, 446; main text, 3000

Tweetable Statement: Innovating stress urinary incontinence evaluation with deep learning! Our study applies deep learning on transperineal ultrasound videos, uncovering bladder neck motion trajectories and parameters, possibly paving the way for tailored intervention.

Short Title: DL-assisted transperineal ultrasound for bladder neck motion in SUI

AJOG at a Glance

A. Why was this study conducted?

- No universally recognized transperineal ultrasound parameters are available for evaluating stress urinary incontinence; commonly used parameters capture limited information that may be insufficient.
- Bladder neck motion is crucial in stress urinary incontinence, yet objective and visual methods to assess its impact are lacking.

B. What are the key findings?

- Deep learning can automatically trace and visualize the bladder neck motion trajectory and has identified three motion parameters: Valsalva duration, average speed of the β angle, and maximum speed of the urethral rotation angle—valuable for diagnosing stress urinary incontinence.

C. What does this study add to what is already known?

- The bladder neck motion trajectory during the Valsalva maneuver can be visualized.
- Three motion parameters were identified as novel diagnostic parameters for stress

urinary incontinence.

- Deep learning may provide a novel approach for the diagnosis and efficacy evaluation of stress urinary incontinence.

Abstract

BACKGROUND: No universally recognized transperineal ultrasound parameters are available for evaluating stress urinary incontinence. The information captured by commonly used perineal ultrasound parameters is limited and insufficient for a comprehensive assessment of stress urinary incontinence. Although bladder neck motion plays a major role in stress urinary incontinence, objective and visual methods to evaluate its impact on stress urinary incontinence remain lacking.

OBJECTIVE: To use a deep learning–based system to evaluate bladder neck motion using two-dimensional transperineal ultrasound videos, exploring motion parameters for diagnosing and evaluating stress urinary incontinence. We hypothesized that bladder neck motion parameters are associated with stress urinary incontinence and are useful for stress urinary incontinence diagnosis and evaluation.

STUDY DESIGN: This retrospective study including 217 women involved the following parameters: maximum and average speeds of bladder neck descent, β angle, urethral rotation angle, and duration of the Valsalva maneuver. The fitted curves were derived to visualize bladder neck motion trajectories. Comparative analyses were conducted to assess these parameters between stress urinary incontinence and control groups. Logistic regression and receiver operating characteristic curve analyses were employed to evaluate the diagnostic performance of each motion parameter and their combinations for stress urinary incontinence.

RESULTS: Overall, 173 women were enrolled in this study (82, stress urinary incontinence group; 91, control group). No significant differences were observed in the maximum and average speeds of bladder neck descent and in the speed variance of bladder neck descent. The maximum and average speed of the β and urethral rotation angles were faster in the stress urinary incontinence group than in the control group (151.2 vs 109.0 mm/s, *P*=0.001; 6.0 vs 3.1 mm/s, *P* <0.001; 105.5 vs 69.6 mm/s, *P* <0.001; 10.1 vs 7.9 mm/s, *P*=0.011, respectively). The speed variance of the β and urethral rotation angles were higher in the stress urinary incontinence group (844.8 vs 336.4, *P* <0.001; 347.6 vs 131.1, *P* <0.001, respectively). The combination of the average speed of the β angle, maximum speed of the urethral rotation angle, and duration of the Valsalva maneuver demonstrated a strong diagnostic performance (area under the curve, 0.87). When $0.481*\beta\ angle_{a} + 0.013*URA_{m} + 0.483*D_{val} = 7.405$, the diagnostic sensitivity was 70% and specificity was 92%, highlighting the significant role of bladder neck motion in stress urinary incontinence, particularly changes in the speed of the β and urethral rotation angles.

CONCLUSIONS: A system utilizing deep learning can describe the motion of the bladder neck in women with stress urinary incontinence during the Valsalva maneuver, making it possible to visualize and quantify bladder neck motion on transperineal ultrasound. The speeds of the β and urethral rotation angles and duration of the Valsalva maneuver were relatively reliable diagnostic parameters.

Keywords: transperineal ultrasound; stress urinary incontinence; deep learning; bladder neck motion

Introduction

Stress urinary incontinence (SUI) is defined as involuntary urination on physical exertion or sneezing or coughing; 23%–44% of women experience urinary incontinence, with approximately 50% being SUI cases. [1-3] The highest incidence occurs in women over 55, making it a common health issue.[2,3]

Bladder neck (BN) mobility plays an important role in SUI.[4-6] However, observing the entire process of BN motion objectively and comprehensively remains difficult. This is mainly because SUI results from a complex interplay of pelvic floor muscles, nerves, hormones, and other factors.[4,5,7] Moreover, the motion is fast, making it challenging to visualize and quantify. Currently, the SUI diagnosis is largely subjective, and management decisions are best assessed through subjective reporting.[5,8] However, subjective evaluation provides limited information about the underlying pathophysiology, potentially missing opportunities for personalized treatments.

MRI can be used to study the pelvic floor structure and detect abnormalities, but observing BN motion is complex, time-consuming, and requires high patient compliance.[9] Transperineal ultrasound (TPUS) is highly recommended for evaluating SUI owing to its advantages of visualizing pelvic morphology, ease of access, non-invasiveness, and cost-effectiveness.[10-12] TPUS is often conducted with the Valsalva maneuver, which simulates increased abdominal pressure. This allows for measuring these traditional parameters such as bladder neck descent (BND), β angle, and urethral rotation angle (URA) both at rest and the end of the Valsalva maneuver (Figure 1), helping assess BN mobility and evaluate SUI.[6,13,14] However, the diagnostic performance of these parameters varies across studies.[13-15] This inconsistency is possibly due to the complex pathophysiology of SUI not being fully understood with TPUS. Additionally, TPUS primarily evaluates SUI at two static moments (at rest and the end of the Valsalva maneuver), leaving BN motion during the Valsalva largely unexplored. This limits the accurate assessment of BN motion and evaluation of treatment efficacy for SUI.

Deep learning (DL) has significantly improved clinical workflows.[16-18] DL-based TPUS methods have shown high efficiency and reliability in puborectalis muscle and levator hiatus segmentation.[19,20] It has also been proven to be an easy and efficient tool for assessing spatial and temporal displacement, opening up the possibility of using DL to automatically capture BN motion.[17,18]

In this study, we innovatively used a DL-based system to analyze two-dimensional (2D) TPUS videos, investigate BN motion in women with SUI, and explore BN motion parameters for evaluating SUI. We hypothesized that BN motion parameters are associated with SUI and are useful for SUI diagnosis.

Methods

Study Design and Participants

This retrospective study included 217 women referred to Zhejiang Provincial People's Hospital for pelvic floor dysfunction or postpartum visits between December 2022 and September 2023. The Institutional Review Board of Zhejiang Provincial People's Hospital approved the study (number JS2022038). Women who underwent routine interviews, physical examinations, and TPUS examinations were included. 2D TPUS videos during the Valsalva maneuver were typically recorded as part of routine clinical practice. Data on age, height, weight, parity, menopausal status, and history of gynecologic or pelvic surgical procedures were retrieved from the electronic medical system; 2D TPUS videos were retrieved from the Ultrasound Medicine Department. Women diagnosed with SUI by urologists or gynecologists were included in the SUI group. Healthy continent women were included in the control group. We excluded women with a history of treatment of SUI or pelvic surgery, who were unable to perform Valsalva even in the standing position or persistently coexisted with levator coactivation, or who had pelvic organ prolapse beyond the hymen. Women with unqualified 2D TPUS videos, including those with incomplete recordings of the Valsalva maneuver or videos not showing important anatomical landmarks (such as the pubic symphysis, urethra, or BN), were also excluded.

TPUS

TPUS was performed using a Voluson E8 device (GE Healthcare, Chicago, IL) with a 4–8-MHz 4-dimensional volume transducer. Two radiologists with > 3 years of TPUS experience performed the examination per the AIUM/IUGA.[10] The midsagittal plane was acquired with the visualized pubic symphysis, urethra, bladder, vagina, and rectum. All women were in the dorsal lithotomy position or the standing position after bladder voiding. The Valsalva maneuver was performed at least thrice, and videos of the maximal Valsalva maneuver were selected.

Development of DL-Based AutoPelvic System

The DL-based AutoPelvic system (RayShape Medical Technology, Shenzhen, China) was used to analyze BN motion using 2D TPUS videos. The system has been approved with the National Medical Products Administration certificate. The DL algorithm, which was proposed in our previous work, was integrated into the AutoPelvic system (Supplementary Methods)[21]. The algorithm is based on Deeplabv3+ (Supplementary Figures) and was built on a large training dataset, covering nearly 1000 TPUS videos from machines of GE Healthcare, Mindray, Philips, and Edan at five hospitals, with > 40,000 images.[22].

The DL-based AutoPelvic system (Videoclips) provided BND, β angle, and URA at each frame. The duration of Valsalva (D_{val}) in each video and fitted curves of each motion parameter were generated from the system as well. Fitted curves were used to visualize trajectories of these motion parameters between groups. Each curve represents the BN motion parameters of all women in each group during Valsalva. As different women have different D_{val}, we used the percentage of D_{val} as the X-axis and parameter values as the Y-axis. The Locally Weighted Scatterplot Smoothing algorithm was applied to smooth these curves.

2D TPUS Video Analysis

Based on the BND, β angle, and URA at each frame provided by the AutoPelvic system, the motion parameters included the maximum and average speed of BND (BND_m, BND_a), β angle (β $angle_m$, β $angle_a$), and URA (URA_m, URA_a), respectively, D_{val} and speed variance during Valsalva was calculated (Figures 2, 3). Speed variance was used to compare speed variations between groups. It can reflect the smoothness of motion trajectories.

Cystocele and SUI can coexist owing to shared common risks.[23,24] To further explore SUI pathophysiological mechanisms on whether cystocele affects BN motion in SUI, we conducted a subgroup analysis comparing women with and without cystocele in the SUI group. Cystocele was defined as the descent of the bladder to ≥ 10 mm below the pubic symphysis reference line during the Valsalva maneuver. This value aligns with stage 2 in the POP-Q classification and indicates significant prolapse.[25]

Statistical Analysis

SPSS (version 26, Chicago, IL) was used. Continuous and categorical data are presented as mean ± standard deviation and number (percentage), respectively. Normality data distribution was evaluated with the Kolmogorov–Smirnov test. Independent-sample t-test and the Mann–Whitney U test were used to compare normally distributed and skewed variables. Categorical data were compared with the chi-square test. Associations between motion parameters and SUI were evaluated using multivariable logistic regression. The receiver operating characteristic (ROC) curve analysis was applied to calculate the area under the ROC curve (AUC) to evaluate the diagnostic ability of each motion parameter for SUI. To select the best combination of motion parameters for SUI, binary logistic regression was applied to calculate the predictive probability of combined parameters. ROC curves were applied to calculate

AUCs using predictive probabilities as covariates to estimate the diagnostic ability of each combination for SUI.[26] $P < 0.05$ (two-sided) indicated statistical significance.

Results

Of 217 women, we excluded 16 (7.4%) owing to unqualified videos; 12 (5.5%), insufficient Valsalva or levator ani coactivation; 7 (3.2%), severe pelvic organ prolapse beyond the hymen; 5 (2.3%), previous or current SUI treatment; and 4 (1.8%), pelvic surgery. Of the remaining 173, 82 (47.4%) were included in the SUI group and 91 (52.6%) in the control group (Table 1). A significant difference was observed between the two groups in age, parity, body mass index (BMI), and menopause. Women in the SUI group were older (42.0 vs 34.4), had higher BMIs (24.8 vs 23.8), and parity (1.3 vs 1.6) than women in the control group. BND_m, BND_a, and speed variance of BND was not significantly different between groups. However, significant differences were found in β $angle_m$, β $angle_a$, URA_m, and URA_a (151.2 vs 109.0 mm/s, P=0.001; 6.0 vs 3.1 mm/s, P<0.001; 105.5 vs 69.6 mm/s, P<0.001; 10.1 vs 7.9 mm/s, P=0.011, respectively). Speed variance of the β angle and URA also showed significant differences between groups (844.8 vs 336.4, P <0.001;347.6 vs 131.1, P<0.001, respectively). D_{val} was 7.8 and 6.1 s in the SUI and control groups, respectively (P<0.001). No significant differences were found in motion parameters between women with cystoceles and without cystoceles (Supplementary Table 1).

Fitted curves were used to visualize the β angle, URA, and BND over time during the Valsalva maneuver (Figure 4). BND in women with SUI was generally higher than that in continent women. Similarly, the β angle and URA tended to be larger than those in the control group. The curves in the second row show changes in speed over time, revealing that speeds of the BN, β angle, and URA were faster in the SUI group. All parameters reached their maximal speed at around 20% of D_{val}.

In multivariable regression analysis, after adjusting for age, BMI, parity, and menopause, the odds ratio (OR) for SUI by motion parameters is presented in Table 2. β $angle_m$ (OR 1.01 [95% confidence interval 1.00–1.02], P=0.005), β $angle_a$ (1.40 [1.19–1.63], P<0.001), URA_m (1.02 [1.01–1.03], P<0.001), URA_a (1.08 [1.01–1.16], P=0.027), and D_{val} (1.24 [1.09–1.41], P=0.001) were significant diagnostic parameters. AUCs of β $angle_m$, β $angle_a$, URA_m, URA_a, and D_{val} were 0.67, 0.74, 0.72, 0.60, and 0.66, respectively (Table 3, Figure 5a). β $angle_a$ + URA_m had an AUC of 0.75; β $angle_a$ + URA_m + D_{val}, 0.87; β $angle_a$ + URA_m + URA_a, 0.78; and β $angle_a$ + URA_m + β $angle_m$, 0.75, indicating that URA_a and β $angle_m$ had limited significant diagnostic ability (Table 3, Figure 5b). When β $angle_a$, URA_m, and D_{val} were combined to diagnose SUI, they showed better performance (AUC, 0.87) than those generated based on each motion parameter individually. Table 3 also shows the fitted equation derived from binary logistic analysis and ROC analysis for the combination of β $angle_a$, URA_m and D_{val}. When 0.481*β $angle_a$ + 0.013*URA_m + 0.483*D_{val} = 7.405, the diagnostic sensitivity was 70% and specificity was 92%.

Comment

Principle Findings

In this retrospective study, we utilized DL to analyze BN motion using 2D TPUS videos in women with SUI. The DL algorithm automatically generated the speed for BND, β angle, and URA over time. We investigated BN motion parameters (BND_m, BND_a, β $angle_m$, β $angle_a$, URA_m) of women with SUI and compared them with those of continent women, leading to three main findings.

First, during the Valsalva maneuver, the maximum and average speeds of β angle and URA in the SUI group were faster than those in the control group. Speed variability of the β angle and URA were greater than those in the control group, implying the support around the BN and proximal urethra is stronger in continent women than in those with SUI. However, BND_m and BND_a were not significantly associated with SUI in our study even after adjusting for age, BMI, parity, and menopause, possibly owing to that the morphology of the trigone and proximal urethra junction is more crucial than distance for maintaining urinary continence.

Second, the maximal speed of BND, β angle, and URA all reached around 20% of D_{val}, suggesting that the BN and proximal urethra are also a kinematic junction, potentially affecting each other's movement during the Valsalva. No significant impact of cystocele was observed on BN motion parameters in women with SUI.

Third, the combination of β $angle_a$, URA_m, and D_{val} was selected as best diagnostic parameters: sensitivity was 70% and specificity was 92%, with an AUC of 0.87.

Results in the Context of What is Known

To our knowledge, this is the first study using DL to investigate potential associations between TPUS motion parameters and SUI. Despite those traditional parameters having been used for two decades, they provided limited information. The BN motion has been overlooked owing to the absence of applicable tracking tools.

Several methods have been proposed to evaluate BN motion in women with SUI using TPUS. Rahmanian et al.[27] and Peng et al.[28] combined TPUS with a six-degrees-of-freedom measurement device and the Flock of Birds system to observe BN motion, demonstrating its significant value in SUI assessment. However, the method was complex and not suitable for clinical practice as it requires specialized devices, coordinate systems, and expertise. Their studies only observed the motion process during coughing in nine women with SUI and did not observe changes in β angle and URA. Pirpiris et al.,[29] Dong et al.,[30] and Zhao et al.,[31] used several equidistant points to manually segment the urethra to establish urethral motion profiles. They measured these points at rest and the end of Valsalva, and then manually calculated the motion of these equidistant points. However, this method is time-consuming and may vary significantly between different operators. Additionally, the motion of the BN and urethra is a continuous process; discrete measurements are not enough to capture the motion.

In recent years, DL techniques have been developed rapidly. By utilizing convolutional and recurrent neural networks, DL algorithms can automatically extract and identify features representing motion and depth information, effectively capturing spatial and temporal information from video sequences.[16-19] This makes it possible to visualize information probably invisible to human eyes. The application of DL algorithms facilitated the real-time acquisition of D_{val} rather than relying on multiple manual measurements to determine start and end points of the Valsalva maneuver.[32]

D_{val} was longer (7.8 s) in the SUI than in the control group (6.1 s), suggesting that women with SUI might need to sustain the Valsalva maneuver for a longer duration to achieve a more comprehensive assessment. This result supports the findings from Orejuela et al.[32] that the Valsalva maneuver should last at least 6 s.

Concerning cystocele in SUI, no significant differences were observed in motion parameters between the two groups. This might be due to the limited number of SUI patients with cystocele (n=26) or this might also suggest that the BN motion during the Valsalva maneuver is similar between SUI patients with and without cystocele, indicating that the presence of cystocele does not affect underlying mechanisms of BN motion in SUI.

Combination motion parameters had better performance than traditional parameters. A previous study reported an AUC of 0.61 for diagnosing urodynamic stress incontinence using BND.[6] In our study, the AUC for each single motion parameter was 0.60–0.74, indicating each parameter remains relatively valuable for diagnosing SUI. The combination of the β $angle_a$, URA_m, and D_{val} demonstrated strong diagnostic performance (AUC 0.87) and exhibited high specificity (92%), suggesting BN motion parameters play a more significant role in ruling out SUI, thereby avoiding unnecessary invasive examinations and preventing overtreatment.

Women in the SUI group exhibited faster speeds of BN angles, with all speeds reaching their maximum at almost the same time. The BN and proximal urethra may have specific motion characteristics during the Valsalva maneuver. This finding is consistent with the swinging theory proposed by Routzong et al.[33,34] They found that the BN in women with SUI exhibited a greater swinging amplitude than that in continent women. This swinging is part of the passive urethral closure mechanism and that we attribute the increased swinging to the weakened integrity of the connective tissue around the BN.[33,34] This suggests that evaluating the motion of the BN and proximal urethra together, rather than separately, can provide a more comprehensive understanding of SUI.

Clinical and Research Implications

We used DL to visualize the spatiotemporal movement of the BN, enabling physicians to better understand changes occurring in this region and providing a new perspective for studying underlying SUI mechanisms. We identified three motion parameters (β $angle_a$, URA_m, and D_{val}) as diagnostic SUI parameters. Their combination outperformed each single one, offering a more comprehensive understanding that SUI is influenced by multiple motion factors.

Moreover, the DL algorithm can simplify TPUS by automatically obtaining all measurements, thereby improving efficiency and reducing operator burden. We established a diagnostic equation, providing a more promising diagnostic method. A deeper understanding of BN motion may pave the way for personalized SUI treatment.

Tailoring interventions based on specific motion patterns can optimize treatment outcomes and aid in more effective SUI management. However, further research is needed to validate and expand the application of these results in the assessment of pelvic floor disorders.

It is important to ensure a sufficient Valsalva maneuver for SUI evaluation. The maximum speed of motion parameters occurs at around 20% of the Valsalva duration, indicating that the abdominal pressure exerted on the BN is most significant initially. Treatments focusing on initial urination control may be a breakthrough for SUI management.

Strengths and Limitations

Regarding strengths, first, it is the first to use DL algorithms to extract BN motion parameters and investigate potential associations between these parameters and SUI. Second, it is the first to visualize the BN motion trajectory during the Valsalva maneuver, revealing potential physiological mechanisms. Third, the DL algorithm simplifies TPUS by automatically obtaining all measurements, improving work efficiency and reducing operator burden.

Regarding limitations, first, this was a single-center study; although DL algorithms were established using multicenter data, future studies should expand the sample size. Second, women in the SUI group were older and had more childbirths compared to those in the control group, the results should be generalized with caution. Third, while we focused on BN motion, others have pointed out that the mid-urethra is also related to SUI. Further research should explore motion patterns of the urethra to better understand SUI. Lastly, SUI is a multifactorial disease, and motion parameters in this study might not fully capture its underlying pathophysiological mechanisms. Future studies should explore additional motion parameters to gain a more comprehensive SUI understanding.

Conclusions

With DL application in TPUS, we found several promising SUI diagnostic parameters: β angle$_a$, URA$_m$, and D$_{val}$—these can be generated automatically via DL algorithms with non-invasive TPUS. Utilizing these parameters enables the BN motion trajectory to be visualized and quantified during the Valsalva maneuver, facilitating a deeper understanding of underlying SUI mechanisms. This approach provides more valuable information, helps simplify and improve clinical work, and enhances efficiency.

Acknowledgments

We thank Prof. Ruobing HUANG, Yan CAO, and Rongbo LING for advice on manuscript writing and revision and Rui GAO for DL algorithm development. We also thank Dr. Juan SUN for coordinating TPUS examinations.

Reference

1. Haylen BT, de Ridder D, Freeman RM, et al. An International Urogynecological Association (IUGA)/International Continence Society (ICS) joint report on the terminology for female pelvic floor dysfunction. *Int Urogynecol J*. Jan 2010;21(1):5-26. doi:10.1007/s00192-009-0976-9
2. Hunskaar S, Lose G, Sykes D, Voss S. The prevalence of urinary incontinence in women in four European countries. *BJU Int*. Feb 2004;93(3):324-30. doi:10.1111/j.1464-410x.2003.04609.x
3. Hannestad YS, Rortveit G, Sandvik H, Hunskaar S, Norwegian EsEoIitCoN-T. A community-based epidemiological survey of female urinary incontinence: the Norwegian EPINCONT study. Epidemiology of Incontinence in the County of Nord-Trondelag. *J Clin Epidemiol*. Nov 2000;53(11):1150-7. doi:10.1016/s0895-4356(00)00232-8
4. Yang X, Wang X, Gao Z, et al. The Anatomical Pathogenesis of Stress Urinary Incontinence in Women. *Medicina (Kaunas)*. Dec 20 2022;59(1)doi:10.3390/medicina59010005
5. Falah-Hassani K, Reeves J, Shiri R, Hickling D, McLean L. The pathophysiology of stress urinary incontinence: a systematic review and meta-analysis. *Int Urogynecol J*. Mar 2021;32(3):501-552. doi:10.1007/s00192-020-04622-9
6. Naranjo-Ortiz C, Shek KL, Martin AJ, Dietz HP. What is normal bladder neck anatomy? *Int Urogynecol J*. Jun 2016;27(6):945-50. doi:10.1007/s00192-015-2916-1
7. Bodner-Adler B, Bodner K, Kimberger O, et al. Role of serum steroid hormones in women with stress urinary incontinence: a case-control study. *BJU Int*. Sep 2017;120(3):416-421. doi:10.1111/bju.13902
8. Abrams P, Cardozo L, Wagg A, Wein A. Incontinence 6th Edition (2017). *International Continence Society, Bristol UK*. 2017;
9. Kumra M, Kachewar S, Lakhkar D. Applications and limitations of magnetic resonance defecography in evaluation of pelvic floor dysfunction disorders. *Int J Radiol Imaging Technol*. 2019;5:045.
10. AIUM/IUGA practice parameter for the performance of Urogynecological ultrasound examinations : Developed in collaboration with the ACR, the AUGS, the AUA, and the SRU. *Int Urogynecol J*. Sep 2019;30(9):1389-1400. doi:10.1007/s00192-019-03954-5
11. Dietz HP. Ultrasound imaging of the pelvic floor. Part I: two-dimensional aspects. *Ultrasound Obstet Gynecol*. Jan 2004;23(1):80-92. doi:10.1002/uog.939
12. Dietz HP, Jarvis SK, Vancaillie TG. The assessment of levator muscle strength: a validation of three ultrasound techniques. *Int Urogynecol J Pelvic Floor Dysfunct*. 2002;13(3):156-9; discussion 159. doi:10.1007/s192-002-8346-5
13. Xiao T, Chen Y, Gan Y, Xu J, Huang W, Zhang X. Can Stress Urinary Incontinence Be Predicted by Ultrasound? *AJR Am J Roentgenol*. Nov 2019;213(5):1163-1169. doi:10.2214/ajr.18.20893
14. Keshavarz E, Pouya EK, Rahimi M, et al. Prediction of Stress Urinary Incontinence Using the Retrovesical (beta) Angle in Transperineal Ultrasound. *J Ultrasound Med*. Aug 2021;40(8):1485-1493. doi:10.1002/jum.15526
15. Hongliang Y, Pengfei L, Cuiping J, Jieqian H, Ling P, Yumin S. Pelvic floor function and morphological abnormalities in primiparas with postpartum symptomatic stress urinary incontinence based on the type of delivery: a 1:1 matched case-control study. *Int Urogynecol J*. Feb 2022;33(2):245-251. doi:10.1007/s00192-021-04816-9

16. Manakitsa N, Maraslidis GS, Moysis L, Fragulis GF. A Review of Machine Learning and Deep Learning for Object Detection, Semantic Segmentation, and Human Action Recognition in Machine and Robotic Vision. *Technologies*. 2024;12(2):15.

17. Xu Y, Liu X, Cao X, et al. Artificial intelligence: A powerful paradigm for scientific research. *The Innovation*. 2021;2(4)

18. Alowais SA, Alghamdi SS, Alsuhebany N, et al. Revolutionizing healthcare: the role of artificial intelligence in clinical practice. *BMC Med Educ*. Sep 22 2023;23(1):689. doi:10.1186/s12909-023-04698-z

19. Szentimrey Z, Ameri G, Hong CX, Cheung RYK, Ukwatta E, Eltahawi A. Automated segmentation and measurement of the female pelvic floor from the mid-sagittal plane of 3D ultrasound volumes. *Med Phys*. Oct 2023;50(10):6215-6227. doi:10.1002/mp.16389

20. van den Noort F, Manzini C, van der Vaart CH, van Limbeek MAJ, Slump CH, Grob ATM. Automatic identification and segmentation of slice of minimal hiatal dimensions in transperineal ultrasound volumes. *Ultrasound Obstet Gynecol*. Oct 2022;60(4):570-576. doi:10.1002/uog.24810

21. Wei NY, Li XK, Lu XD, Liu XT, Sun RJ, Wang Y. Study on the Consistency Between Automatic Measurement Based on Convolutional Neural Network Technology and Manual Visual Evaluation in Intracavitary Ultrasonic Cine of Anterior Pelvic. *J Ultrasound Med*. Apr 2024;43(4):671-681. doi:10.1002/jum.16392

22. Chen L-C, Zhu Y, Papandreou G, Schroff F, Adam H. Encoder-decoder with atrous separable convolution for semantic image segmentation. 2018:801-818.

23. Bu L, Yang D, Nie F, Li Q, Wang YF. Correlation of the type and degree of cystocele with stress urinary incontinence by transperineal ultrasound. *J Med Ultrason (2001)*. Jan 2020;47(1):123-130. doi:10.1007/s10396-019-00972-0

24. Yalcin OT, Yildirim A, Hassa H. The effects of severe cystocele on urogynecologic symptoms and findings. *Acta Obstet Gynecol Scand*. May 2001;80(5):423-7.

25. Dietz HP, Kamisan Atan I, Salita A. Association between ICS POP-Q coordinates and translabial ultrasound findings: implications for definition of 'normal pelvic organ support'. *Ultrasound in Obstetrics & Gynecology*. 2016;47(3):363-368. doi:https://doi.org/10.1002/uog.14872

26. Yang Q, Zhang P, Wu R, Lu K, Zhou H. Identifying the Best Marker Combination in CEA, CA125, CY211, NSE, and SCC for Lung Cancer Screening by Combining ROC Curve and Logistic Regression Analyses: Is It Feasible? *Dis Markers*. 2018;2018:2082840. doi:10.1155/2018/2082840

27. Rahmanian S, Jones R, Peng Q, Constantinou CE. Visualization of biomechanical properties of female pelvic floor function using video motion tracking of ultrasound imaging. *Stud Health Technol Inform*. 2008;132:390-5.

28. Peng Q, Jones R, Shishido K, Constantinou CE. Ultrasound evaluation of dynamic responses of female pelvic floor muscles. *Ultrasound Med Biol*. Mar 2007;33(3):342-52. doi:10.1016/j.ultrasmedbio.2006.08.020

29. Pirpiris A, Shek KL, Dietz HP. Urethral mobility and urinary incontinence. *Ultrasound Obstet Gynecol*. Oct 2010;36(4):507-11. doi:10.1002/uog.7658

30. Dong B, Shi Y, Chen Y, Liu M, Lu X, Liu Y. Perineal ultrasound to assess the urethral spatial movement in stress urinary incontinence in women. *BMC Urol*. Mar 27 2023;23(1):44. doi:10.1186/s12894-023-01220-x

31. Zhao B, Wen L, Liu D, Huang S. Urethral configuration and mobility during urine leaking described using real-time transperineal ultrasonography. *Ultrasonography*. Jan 2022;41(1):171-176. doi:10.14366/usg.21058

32. Orejuela FJ, Shek KL, Dietz HP. The time factor in the assessment of prolapse and levator ballooning. *Int Urogynecol J*. Feb 2012;23(2):175-8. doi:10.1007/s00192-011-1533-x

33. Routzong MR, Chang C, Goldberg RP, Abramowitch SD, Rostaminia G. Urethral support in female urinary continence part 1: dynamic measurements of urethral shape and motion. *Int Urogynecol J*. Mar 2022;33(3):541-550. doi:10.1007/s00192-021-04765-3

34. Routzong MR, Martin LC, Rostaminia G, Abramowitch S. Urethral support in female urinary continence part 2: a computational, biomechanical analysis of Valsalva. *Int Urogynecol J*. Mar 2022;33(3):551-561. doi:10.1007/s00192-021-04694-1

Table 1 Comparison of demographic data and BN motion parameters between the SUI and control groups

	SUI (n = 82)	**Control (n = 91)**	***P*-value**
Demographic data			
Age (years)	42.0 ± 13.1	32.4 ± 7.5	<0.001
BMI (kg/m^2)	24.8 ± 2.3	23.8 ± 2.8	0.020
Parity	1.6 ± 0.7	1.3 ± 0.5	<0.001
Menopause	19 (23.2%)	4 (0.4%)	<0.001
Motion parameters			
BND_m (mm/s)	40.8 ± 26.3	34.0 ± 22.1	0.065
Timing of reaching BND_m relative to D_{val} (%)	20.3 ± 18.6	21.8 ± 19.1	0.603
BND_a (mm/s)	4.7 ± 2.2	5.2 ± 2.6	0.220
β $angle_m$ (°/s)	151.2 ± 77.5	109.0 ± 71.3	0.001
Timing of reaching β $angle_m$ relative to D_{val} (%)	30.4 ± 23.5	27.8 ± 24.5	0.504
β $angle_a$ (°/s)	6.0 ± 3.8	3.1 ± 2.3	<0.001
URA_m (°/s)	105.5 ± 55.2	69.6 ± 45.0	<0.001
Timing of reaching URA_m relative to D_{val} (%)	25.6 ± 22.4	24.3 ± 20.5	0.680

URA_a (°/s)		10.1 ± 6.5	7.9 ± 4.3	0.011
Speed variance	BND	38.4 ± 35.2	30.8 ± 21.6	0.125
	β angle	844.8 ± 676.1	336.4 ± 273.2	<0.001
	URA	347.6 ± 284.0	131.1 ± 96.5	<0.001
D_{val} (s)		7.8 ± 3.7	6.1 ± 2.3	<0.001

BMI, body mass index; BN, bladder neck; BND_m and BND_a, maximum and average speed of bladder neck descent, respectively; β $angle_m$, β $angle_a$, URA_m, and URA_a, maximum and average speed of the β and urethral rotation angles, respectively; D_{val}, duration of Valsalva; SUI, stress urinary incontinence

Data presented as mean ± standard deviation for continuous variables or number (percentage) for categorical variables

P-values reported using the Independent-sample t-test and Mann–Whitney U test for continuous variables and the chi-square test for categorical variables

Table 2 Multivariable logistic regression analysis of BN motion parameters in SUI

Motion parameters	**Adjusted OR[a] (95% CI)**	***P*-value**
BND_m	1.01 (0.99–1.02)	0.437
BND_a	0.87 (0.75–1.02)	0.087
β $angle_m$	1.01 (1.00–1.02)	0.005
β $angle_a$	1.40 (1.19–1.63)	<0.001
URA_m	1.02 (1.01–1.03)	<0.001
URA_a	1.08 (1.01–1.16)	0.027
D_{val}	1.24 (1.09–1.41)	0.001

BN, bladder neck; BND_m and BND_a, maximum and average speed of bladder neck descent, respectively; β $angle_m$, β $angle_a$, URA_m, and URA_a, maximum and average speed of the β and urethral rotation angles, respectively; CI, confidence interval; D_{val}, duration of Valsalva; OR odds ratio; SUI, stress urinary incontinence

[a] Adjusted for age, body mass index, parity, and menopause

Table 3 Performance of BN motion parameters in the diagnosis of SUI

Motion parameters	**AUC (95% CI)**	**Cutoff**	**Sensitivity**	**Specificity**
β $angle_m$ (°/s)	0.67 (0.58–0.75)	163.1	43%	84%
β $angle_a$ (°/s)	0.74 (0.66–0.82)	3.7	76%	62%
URA_m (°/s)	0.72 (0.63–0.81)	78.2	67%	73%
URA_a (°/s)	0.60 (0.51–0.70)	8.1	59%	66%
D_{val} (s)	0.66 (0.57–0.75)	6.2	71%	57%
β $angle_a$ + URA_m	0.75 (0.67–0.83)	0.280* β $angle_a$ + 0.009* URA_m = 2.617	57%	85%
β $angle_a$ + URA_m + D_{val}	0.87 (0.81–0.93)	0.481*β $angle_a$ + 0.013* URA_m + 0.483 *D_{val} = 7.405	70%	92%
β $angle_a$ + URA_m+URA_a	0.78 (0.70–0.85)	0.387*β $angle_a$ + 0.013 *URA_m – *0.147*URA_a = 2.344	75%	61%

β $angle_a$ + URA_m + β $angle_m$	0.75 (0.67–0.83)	0.269*β $angle_a$ + 0.008*URA_m + 0.001*β $angle_m$ = 2.578	59%	75%

AUC, area under the curve; BN, bladder neck; BND_m and BND_a, maximum and average speed of bladder neck descent, respectively; β $angle_m$, β $angle_a$, URA_m, and URA_a, maximum and average speed of the β and urethral rotation angles, respectively; CI, confidence interval; D_{val}, duration of Valsalva; SUI, stress urinary incontinence

Supplementary Table 1 Comparison of demographic data and BN motion parameters between women with cystocele and without cystocele in the SUI group

	Women with cystoceles (n = 26)	**Women without cystocele (n = 56)**	***P*-value**
Demographic data			
Age (years)	36.1 ± 9.8	44.1 ± 13.5	0.016
BMI (kg/m^2)	24.4 ± 2.3	24.9 ± 2.4	0.377
Parity	1.4 ± 0.5	1.7 ± 0.7	<0.001
Menopause	2 (9.1%)	17 (28.3%)	0.088
Motion parameters			
BND_m (mm/s)	47.3 ± 19.3	38.6 ± 28.1	0.190
Timing of reaching BND_m relative to D_{val} (%)	21.0 ± 20.6	20.0 ± 18.0	0.603
BND_a (mm/s)	5.1 ± 2.3	4.6 ± 2.2	0.380
β $angle_m$ (°/s)	165.0 ± 73.4	146.3 ± 79.0	0.385
Timing of reaching β $angle_m$ relative to D_{val} (%)	32.1 ± 24.1	25.4 ± 21.4	0.299
β $angle_a$ (°/s)	6.0 ± 3.3	6.0 ± 4.1	0.986
URA_m (°/s)	118.7 ± 47.4	101.4 ± 57.1	0.247

Timing of reaching URA_m relative to D_{val} (%)		21.8 ± 16.5	27.0 ± 24.2	0.382
URA_a (°/s)		11.4 ± 6.6	9.6 ± 6.5	0.276
Speed variance	BND	52.5 ± 56.9	35.3 ± 26.0	0.105
	β angle	1021.0 ± 632.4	802.3 ± 684.6	0.265
	URA	407.8 ± 248.3	336.5 ± 292.8	0.395
D_{val} (s)		8.8 ± 3.7	7.5 ± 3.4	0.299

BMI body mass index; BN, bladder neck; BND_m and BND_a, maximum and average speed of bladder neck descent, respectively; β $angle_m$, β $angle_a$, URA_m, and URA_a, maximum and average speed of the β and urethral rotation angles, respectively; D_{val}, duration of Valsalva; SUI, stress urinary incontinence

Data presented as mean ± standard deviation for continuous variables or number (percentage) for categorical variables

P-values reported using the Independent-sample t-test and Mann–Whitney U test for continuous variables and the chi-square test for categorical variables

Figure legends

Figure 1 Schematic diagram of the traditional TPUS parameters

Horizontal solid line: reference line at the inferior–posterior margin of the symphysis pubis. Horizontal dotted line: bladder neck position at rest. 0, at rest; v, at Valsalva. Arrow (0) and Arrow (v): direction of the proximal urethra at rest and Valsalva, respectively.

BNP, bladder neck position; BND, bladder neck descent: difference between the bladder neck to the inferior–posterior margin of the symphysis pubis during Valsalva and at rest; β angle, angle between the proximal urethra and trigone; URA, urethral rotation angle: rotation angle of the proximal urethra during Valsalva; SP, symphysis pubis.

Figure 2 Formulas for BND_m, BND_a, β $angle_m$, β $angle_a$, URA_m, and URA_a calculations

0, at rest; v, at Valsalva. Arrow (0) and Arrow (v): direction of the proximal urethra at rest and Valsalva, respectively. Max: maximum of the parameters; t_0 and t_v: time at rest and Valsalva, respectively. n: number of video frames, $\overline{x}$: average speed, x_k: value of each observation.

BND_m and BND_a, maximum and average speed of bladder neck descent, respectively; BNP, bladder neck position; β $angle_m$, β $angle_a$, URA_m and URA_a, maximum and average speed of the β and urethral rotation angles, respectively; D_{val}, duration of Valsalva; SP, symphysis pubis.

Figure 3 Examples of two women from the SUI and control groups during the Valsalva maneuver

The BN motion curves are shown below the TPUS images. BN, bladder neck; BND, bladder neck descent; D_{val}, duration of Valsalva; SP, symphysis pubis; SUI, stress urinary incontinence; TPUS, transperineal ultrasound; URA, urethral rotation angle.

Figure 4 Fitted curves ± standard deviation of BN motion parameters during Valsalva

Each curve represents BN motion parameters of all women in each group during Valsalva. As different women have different D_{val}, we used the percentage of D_{val} as the X-axis and parameter values as the Y-axis. Red line: fitted curves of the SUI group; green line: fitted curves of the control group. a, b, and c are fitted curves of BND, β angle, and URA during Valsalva, respectively; d, e, and f are fitted curves of BND speed, β angle speed, and URA speed during Valsalva, respectively.

BN, bladder neck; BND, bladder neck decent; D_{val}, duration of Valsalva; SUI, stress urinary incontinence; URA, urethral rotation angle.

Figure 5 ROC curves of BN motion parameters in the diagnosis of SUI

a, ROC curves of the performance of every single motion parameter in diagnosing SUI.

b, ROC curves of the performance of combinations of motion parameters in diagnosing SUI

BN, bladder neck; ROC, receiver operating characteristic; β $angle_m$, β $angle_a$, URA_m, and URA_a, maximum and average speed of the β and urethral rotation angles, respectively; D_{val}, duration of Valsalva; SUI, stress urinary incontinence.

Supplementary Figure 1 Framework of the deep learning–based AutoPelvic system, which used DeepLabV3+ to measure motion parameters automatically: (1) automatically locate landmarks at every frame, (2) measure the BNP for every frame to identify the rest frame and maximal Valsalva frame, and (3) measure BND, β angle, and URA.

BND, bladder neck descent; BNP, bladder neck position; URA, urethral rotation angle. Point S, inferior–posterior border of the symphysis pubis; point U, bladder neck; point E, direction of the proximal urethra; UE, proximal urethra; UP, posterior wall of the bladder.

Supplementary Figure 2 Architecture of DeeplabV3+ for locating landmarks

Videoclips 1, 2 Examples of automatic measurement during TPUS using the AutoPelvic system. 1, a TPUS of the control group; 2, a TPUS of the SUI group.

TPUS, transperineal ultrasound; SUI, stress urinary incontinence.

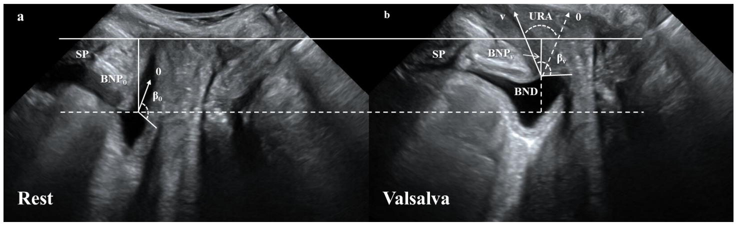
a
SP
BNP$_0$
0
β_0
Rest
b
v
URA
0
SP
BNP$_v$
β_v
BND
Valsalva

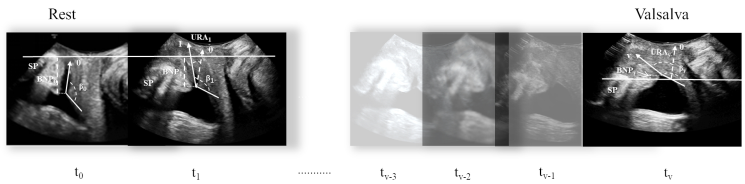

$BND_m = Max(BND_k) = Max\left(\frac{BND_{k-1} - BND_k}{t_k - t_{k-1}}\right)$ $\quad BND_a = \frac{BND_0 - BND_v}{t_v - t_0}$ $\quad D_{val} = t_v - t_0$

$\beta\ angle_m = Max(\beta_k) = Max\left(\frac{\beta_{k-1} - \beta_k}{t_k - t_{k-1}}\right)$ $\quad \beta\ angle_a = \frac{\beta_v - \beta_0}{t_v - t_0}$

$URA_m = Max(URA_k) = Max\left(\frac{URA_{k-1} - URA_k}{t_k - t_{k-1}}\right)$ $\quad URA_a = \frac{URA_v - URA_0}{t_v - t_0}$

Speed variance: $\sum(x_k - \overline{x})$^2/n−1 $\quad$ k $\in (1, v)$

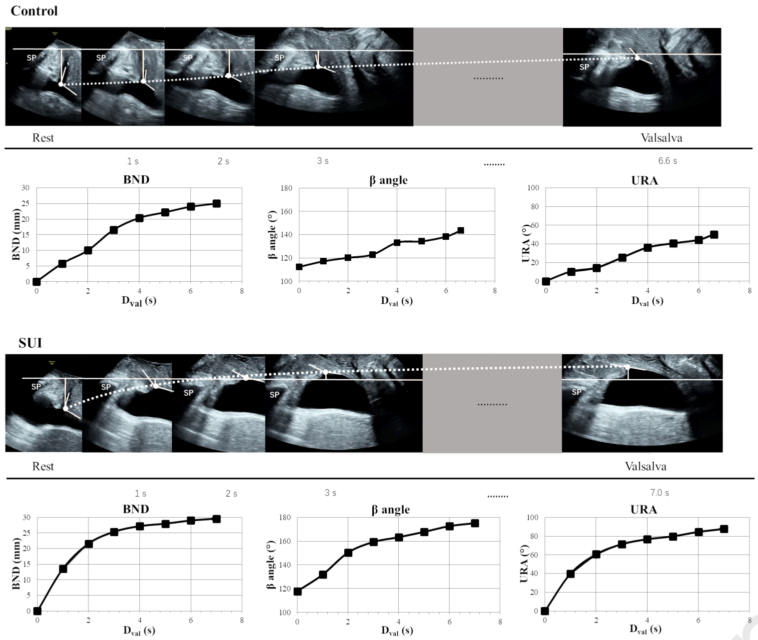
Control
SP
Rest
Valsalva
1 s
2 s
3 s
6.6 s
BND
BND (mm)
β angle
β angle (°)
URA
URA (°)
Dval (s)
SUI
Rest
Valsalva
1 s
2 s
3 s
7.0 s
BND
BND (mm)
β angle
β angle (°)
URA
URA (°)
Dval (s)

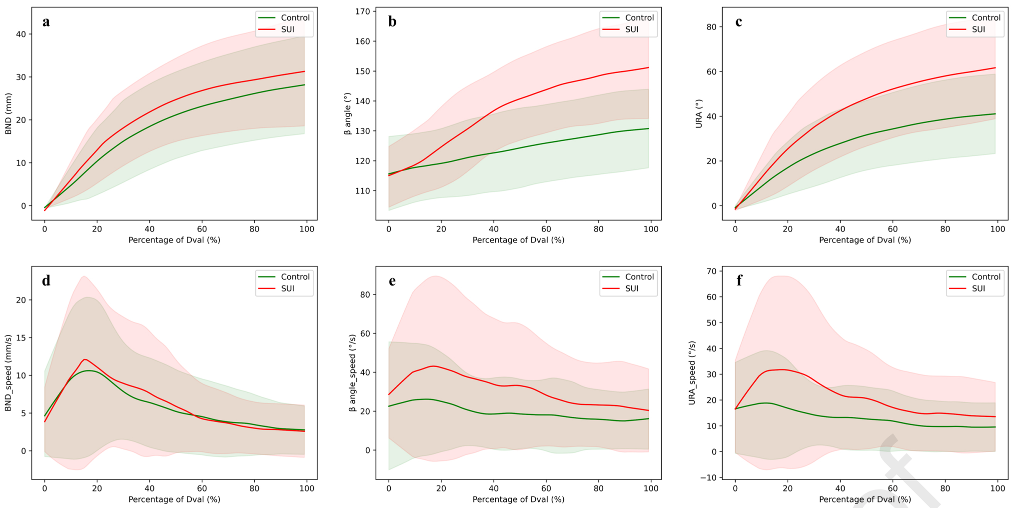
a
b
c
d
e
f
Control
SUI
BND (mm)
β angle (°)
URA (°)
BND_speed (mm/s)
β angle_speed (°/s)
URA_speed (°/s)
Percentage of Dval (%)

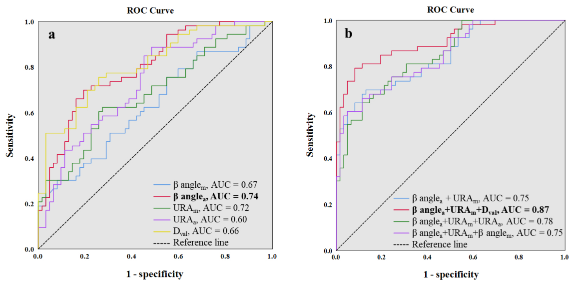
ROC Curve
a
Sensitivity
1 - specificity
β angle$_m$, AUC = 0.67
β angle$_a$, AUC = 0.74
URA$_m$, AUC = 0.72
URA$_a$, AUC = 0.60
D$_{val}$, AUC = 0.66
Reference line
ROC Curve
b
Sensitivity
1 - specificity
β angle$_a$ + URA$_m$, AUC = 0.75
β angle$_a$+URA$_m$+D$_{val}$, AUC = 0.87
β angle$_a$+URA$_m$+URA$_a$, AUC = 0.78
β angle$_a$+URA$_m$+β angle$_m$, AUC = 0.75
Reference line

AJOG American Journal of Obstetrics & Gynecology

American Journal of Obstetrics & Gynecology

STATEMENT OF AUTHORSHIP

Each author is required to submit a signed Statement of Authorship upon submission. This applies to all submission types including Editorials, Letters to the Editor, etc.

Date: 2024.1.17 **Manuscript # (if available):** _____

Manuscript title: The bladder neck kinetics derived from the deep learning-based 2D transperineal ultrasound videos in the analysis of female stress urinary incontinence

Corresponding author: Litao Sun and Dong Ni

Authors may either sign the same form or submit individually

I am an author on this submission, have adhered to all editorial policies for submission as described in the Information for Authors, attest to having met all authorship criteria, and all potential conflicts of interest / financial disclosures appears on the title page of the submission.

Signatures are required - typed signatures are unacceptable.

Typed or CLEARLY Printed Name: **Jin Wang**

Signature: Jin Wang

Typed or CLEARLY Printed Name: **Xin Yang**

Signature: Xin Yang

Typed or CLEARLY Printed Name: **Yanqing Peng**

Signature: Yanqing Peng

Typed or CLEARLY Printed Name: **Yan Zou**

Signature: Yan Zou

Typed or CLEARLY Printed Name: **Xiduo Lu**

Signature: Xiduo Lu

Typed or CLEARLY Printed Name: **Shuangxi Chen**

Signature: Shuangxi Chen

Typed or CLEARLY Printed Name: **Xiaoyi Pan**

Signature: Xiaoyi Pan

Typed or CLEARLY Printed Name: **Dong Ni**

Signature: Dong Ni

Typed or CLEARLY Printed Name: **Litao Sun**

Signature: Litao Sun

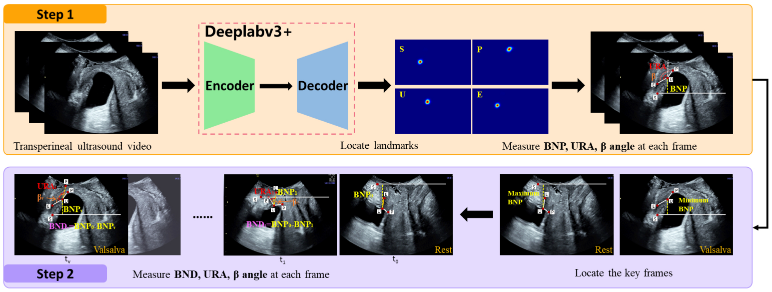
Step 1
Deeplabv3+
Encoder
Decoder
Transperineal ultrasound video
Locate landmarks
Measure BNP, URA, β angle at each frame
Step 2
Measure BND, URA, β angle at each frame
Locate the key frames
Valsalva
Rest
Rest
Valsalva

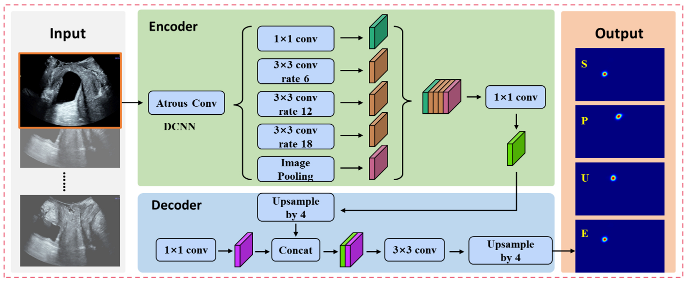
Input
Encoder
Atrous Conv
DCNN
1×1 conv
3×3 conv rate 6
3×3 conv rate 12
3×3 conv rate 18
Image Pooling
1×1 conv
Decoder
Upsample by 4
1×1 conv
Concat
3×3 conv
Upsample by 4
Output
S
P
U
E

Development of Deep Learning (DL)-Based AutoPelvic System

The DL-based AutoPelvic system (RayShape Medical Technology, Shenzhen, China) was used to analyze bladder neck (BN) motion using 2D transperineal ultrasound (TPUS) videos. The system has been approved with the National Medical Products Administration certificate. As shown in Supplementary Figure 1, the DL algorithm, which was proposed in our previous work, was integrated into the AutoPelvic system.[1] The algorithm is based on Deeplabv3+ （Supplemental Figure 1, 2）, a powerful and robust segmentation network.[2]

The DL-based algorithm was built on a large training dataset, covering nearly 1000 TPUS videos from machines of GE healthcare, Mindray, Philips, and Edan at 5 hospitals, with > 40,000 images. The dataset was labeled with point S (the inferior-posterior border of the symphysis pubis), U (the bladder neck), E (the direction of the proximal urethra), and P (the posterior wall of the bladder) by five senior physicians with > 5 years of TPUS experience. We constructed a coordinate system for the image, with the top corner point designated as (0,0). The DL model automatically located these landmarks, and based on their coordinates, we calculated the parameters. The proximal urethra is defined as the section of the urethra near BN. Gauss heatmaps of landmarks were generated according to their coordinates and were used to supervise the output of the algorithm during the training phase.

The AutoPelvic system was fed in TPUS images as input and output the Gauss heatmaps of the landmarks, including points S, U, E, and P, for each frame in the TPUS video. Subsequently, the algorithm automatically measured the bladder neck position (BNP), β angle, and urethral rotation angle (URA) based on the localization of landmarks in every frame. The initiation of the Valsalva maneuver was identified as commencing at the frame with the maximum BNP and ending at the frame with the minimum BNP.

The DL-based AutoPelvic system (Videoclip S1 and S2) provided bladder neck descent (BND), β angle, and URA at each frame. The duration of Valsalva (D_{val}) of each video and the fitted curves of each motion parameter were generated from the system as well. Fitted curves were used to visualize trajectories of these motion parameters between groups. Each curve represents the bladder neck motion parameters of all women in each group during Valsalva. As different women have different D_{val}, we used the percentage of D_{val} as the X-axis and parameter values as the Y-axis. The Locally Weighted Scatterplot Smoothing algorithm was applied to smooth these curves.

On a testing dataset of 400 TPUS videos, the measurements of BND, β angle, and URA by the AutoPelvic system achieved an intraclass correlation coefficient (ICC) of 0.76-0.94 when compared with two senior physicians with > 3 years of TPUS experience.[1]

Our experiments were conducted using PyTorch 1.14.0 on a workstation equipped with an NVIDIA GeForce RTX 3090, utilizing Python for programming.

Reference

1. Wei NY, Li XK, Lu XD, Liu XT, Sun RJ, Wang Y. Study on the Consistency Between Automatic Measurement Based on Convolutional Neural Network Technology and Manual Visual Evaluation in Intracavitary Ultrasonic Cine of Anterior Pelvic. *J Ultrasound Med*. Apr 2024;43(4):671-681. doi:10.1002/jum.16392
2. Chen L-C, Zhu Y, Papandreou G, Schroff F, Adam H. Encoder-decoder with atrous separable convolution for semantic image segmentation. 2018:801-818.